Am J Cancer Res 2025;15(3):1201-1212
www.ajcr.us /ISSN:2156-6976/ajcr0162247

Original Article

Enhanced diagnostic accuracy of contrast-enhanced ultrasound in liver space-occupying lesions: superior sensitivity and specificity over conventional ultrasound

Junfang Wang[1], Weiwei Shi[1], Yuanyuan Jiang[2]

[1]Department of Ultrasound, Central Hospital Affiliated to Shandong First Medical University, Jinan 250013, Shandong, China; [2]Department of Ultrasound Medicine, Shandong Second Provincial General Hospital, Jinan 250022, Shandong, China

Received November 25, 2024; Accepted January 25, 2025; Epub March 15, 2025; Published March 30, 2025

Abstract: Aims: To evaluate the clinical value of contrast-enhanced ultrasound (CEUS) in diagnosing liver space-occupying lesions. Methods: A total of 487 patients with liver space-occupying lesions were examined using both conventional ultrasound and CEUS. The diagnostic results from the two methods were compared, with pathological findings used as the gold standard. Sensitivity, specificity, positive predictive value (PPV), negative predictive value (NPV), and the area under the receiver operating characteristic curve were calculated for each method to assess their diagnostic value. Results: Among the 487 lesions, 220 were malignant and 267 were benign. The relative blood flow (rBF) in the arterial phase of malignant lesions was significantly higher than that of benign lesions, while the rBF in the delayed phase was significantly lower ($P<0.05$). In diagnosing malignant lesions, CEUS had a higher detection rate than conventional ultrasound (75% vs. 43.18%, $P<0.001$). CEUS also demonstrated a higher diagnostic agreement for lesions ≤1 cm compared to conventional ultrasound (85.16% vs. 49.47%, $P<0.001$). The accuracy, sensitivity, specificity, PPV, and NPV of CEUS were all higher than those of conventional ultrasound (all $P<0.05$). Conclusion: CEUS is effective in diagnosing liver space-occupying lesions, with superior sensitivity and specificity compared to conventional ultrasound.

Keywords: Contrast-enhanced ultrasound, liver space-occupying lesions, diagnosis

Introduction

Liver space-occupying lesions (SOLs) refer to abnormal echo regions in the liver parenchyma identified through imaging techniques such as ultrasound or CT, encompassing both benign and malignant lesions. Many patients remain asymptomatic in the early stages of the disease, with clinical symptoms emerging only during the middle to late stages of progression [1]. These lesions are classified into benign and malignant categories. Benign lesions include benign tumors, tumor-like lesions, and hepatic hemangiomas, while malignant lesions primarily consist of liver cancer [2]. Statistics indicate that liver cancer accounts for approximately 45% of global mortality from the disease in China [3]. The treatment options and prognosis for liver SOLs vary significantly between benign and malignant types. Therefore, early diagnosis and accurate differentiation between benign and malignant lesions are crucial for initiating timely treatment and improving patients' quality of life.

Conventional ultrasound (US) has long been a primary imaging method for evaluating liver lesions due to its accessibility, affordability, and real-time imaging capabilities [4]. However, US has limitations in distinguishing between benign and malignant lesions, particularly in complex or ambiguous cases. As a result, additional imaging techniques such as computed tomography (CT) or magnetic resonance imaging (MRI) are often required [5]. Despite their advantages, these modalities have drawbacks, including radiation exposure, higher costs, and limited availability in resource-constrained settings. Contrast-enhanced ultrasound (CEUS) has emerged as an innovative alternative,

https://doi.org/10.62347/BBUT6997

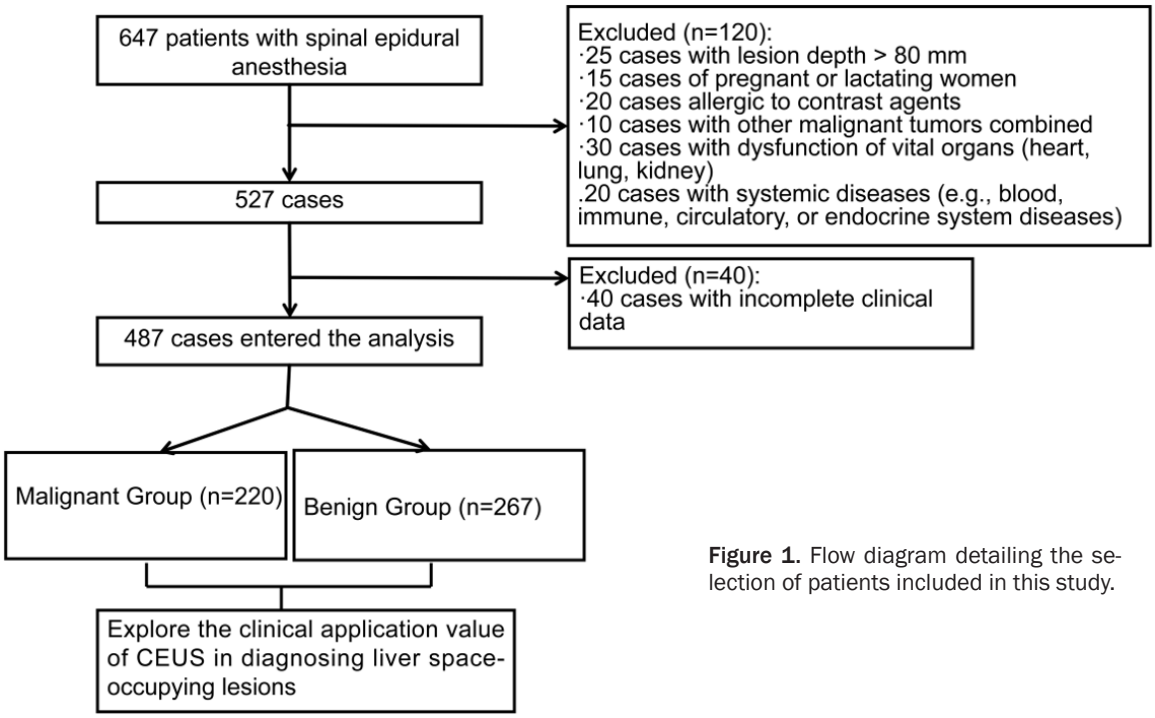

Figure 1. Flow diagram detailing the selection of patients included in this study.

addressing many of the limitations of conventional modalities [6]. CEUS utilizes microbubble-based contrast agents to enhance the visualization of microvascular structures and dynamic perfusion patterns, allowing real-time assessment of lesion vascularity [7]. Unlike CT or MRI, CEUS is radiation-free and non-invasive, making it ideal for patients requiring repeated imaging, such as pregnant women or individuals with chronic liver disease. The dynamic, real-time capabilities of CEUS enable more precise differentiation between benign and malignant lesions, even in small or indeterminate cases [8]. However, despite its potential, the clinical application of CEUS in diagnosing liver SOLs is still evolving, and robust evidence is needed to validate its diagnostic performance. While previous studies have demonstrated the utility of CEUS in specific scenarios like hepatocellular carcinoma (HCC), comparative studies with conventional US remain limited. Furthermore, the diagnostic accuracy of CEUS in distinguishing benign from malignant lesions across diverse populations is not fully established.

This study highlights the unique ability of CEUS to provide real-time dynamic imaging of microvascular perfusion and contrast patterns, representing a significant advancement over conventional US. This innovation allows for more precise differentiation between benign and malignant liver lesions, addressing a critical diagnostic challenge. Clinically, CEUS offers non-invasive, radiation-free imaging, making it especially suitable for vulnerable populations and for frequent follow-ups. By improving diagnostic accuracy and enabling early detection, particularly for small HCCs, CEUS aids in better treatment planning and outcomes. These features underscore the potential of CEUS to transform liver disease management, enhance early intervention strategies, and integrate advanced imaging into routine clinical practice.

Therefore, CEUS was employed in this analysis to explore its clinical value in diagnosing liver SOLs.

Materials and methods

Patient selection

From January 2018 to June 2024, 487 patients with liver SOLs were included in this retrospective study. A total of 487 lesions were examined. The patient selection process is shown in **Figure 1**. This study and its experimental procedures were approved by the Ethics Committee of the Central Hospital Affiliated to Shandong First Medical University.

Inclusion criteria: 1) Patients aged ≥18 years; 2) Diagnosis of both benign and malignant liver lesions confirmed by pathological examination [9]; 3) Patients who underwent routine ultrasound and CEUS examinations at this hospital; 4) No allergies to contrast agents.

Exclusion criteria: 1) Lesions deeper than 80 mm; 2) Pregnant or lactating women; 3) Patients allergic to contrast agents; 4) Patients with concurrent malignant tumors at other sites; 5) Patients with dysfunction of vital organs (e.g., heart, lungs, kidneys); 6) Patients with systemic diseases (e.g., blood, immune, circulatory, or endocrine system disorders); 7) Patients who received systemic chemotherapy or local treatments; 8) Lesions with a diameter of <1 cm; 9) Patients with severe emphysema, pulmonary embolism, or pulmonary arterial hypertension; 10) Patients with severe mental illnesses or consciousness disturbances.

Data extraction

The imaging instruments used were a color Doppler ultrasound diagnostic system (Affiniti 70, Philips Healthcare, Andover, MA, USA) and Siemens Acuson (Siemens Healthineers, Erlangen, Germany). During the CEUS examination, a convex array probe with a frequency of 2.5 to 5.0 MHz was used. The contrast agent, Bracco (Bracco Imaging S.p.A., Milan, Italy), is a sulfur hexafluoride-based microbubble encapsulated by phospholipids. The patient was positioned supine. Initially, a routine ultrasound examination was performed to scan the entire liver, assessing the shape, echogenicity, and other indicators of the target lesion. The largest scanning section of the lesion was selected, and the system was switched to contrast mode with low mechanical index settings.

The contrast agent was dissolved in 5 mL of normal saline and injected via the elbow vein as a bolus within 2 to 3 seconds. The timer was started, and real-time contrast imaging of the lesion and surrounding tissues was observed until the contrast agent was nearly cleared. Dynamic images during the contrast process were stored.

Judgment criteria: Malignant lesions typically show strong enhancement in the arterial phase, followed by a rapid decline in enhancement in the portal venous or delayed phases, exhibiting a “rapid in, rapid out” pattern.

Benign lesions show high or equal enhancement in the arterial phase, with either no change or similar enhancement in the portal venous and delayed phases, or no enhancement in all three phases.

CEUS diagnosis: If the lesion exhibits significant enhancement in the arterial phase and decreased enhancement in the portal venous and delayed phases, it is diagnosed as malignant.

Conventional US examination: Lesions were classified into grades A, B, C, D, and E according to their color patterns.

Grade A: uniform green. Grade B: a mixture of green and blue, with green as the dominant color. Grade C: a mixture of green and blue, with blue as the dominant color. Grade D: blue in the central area. Grade E: entirely blue, with surrounding tissue also showing blue. Grades A and B were classified as benign lesions, while grades C, D, and E were considered malignant lesions.

Outcome measures

Primary outcome measures: The diagnostic efficacy (sensitivity, specificity, and accuracy) of different examination methods was evaluated. Receiver operating characteristic (ROC) curves were used to compare the diagnostic performance of each method.

Secondary outcome measures: The enhancement times for CEUS of SOLs in the liver were compared. This included the initial enhancement time, peak time, duration, and time of initial disappearance.

Statistical analysis

Statistical analysis was performed using SPSS 20.0. Measurement data were presented as mean ± standard deviation. Inter-group comparisons were conducted using the independent samples t-test, and comparisons of rates were performed using the χ^2 test. Sensitivity, specificity, positive predictive value (PPV), and negative predictive value (NPV) were calculated for conventional US and CEUS, respectively. The diagnostic performance of the three methods was assessed using ROC curves. The DeLong test was used to compare the area under the curve (AUC) between CEUS and con-

Table 1. Pathological results of 487 lesions

Nature	Type	Cases, n (%)
Malignant	Hepatocellular carcinoma	177 (36.34)
	Cholangiocellular carcinoma	30 (6.16)
	Mixed tumors	13 (2.67)
Benign	Focal nodular hyperplasia	111 (22.79)
	Hepatic adenoma	96 (19.71)
	Hepatic cystadenoma	38 (7.80)
	Chronic granulomatous disease	22 (4.52)
Total		487 (100)

ventional US to ensure the robustness of the comparison. A significance level of α=0.05 was set, and a *P*-value <0.05 was considered statistically significant.

Results

Pathological results of 487 lesions

Pathological confirmation via biopsy or surgery revealed 220 malignant lesions (45.17%) and 267 benign lesions (54.83%). Among the malignant lesions, 177 were hepatocellular carcinoma (HCC), 30 were cholangiocellular carcinoma (CCC), and 13 were mixed tumors. The benign lesions included 111 cases of focal nodular hyperplasia (FNH), 96 hepatic adenomas (HA), 38 hepatic cystadenomas (HCA), and 22 cases of chronic granulomatous disease (CGD) (**Table 1**).

Demographic data of the two groups

Patients were divided into a malignant group and a benign group according to their pathological results. The malignant group included 220 patients: 162 males (73.64%) and 58 females, aged 35 to 79 years (mean age: 60.95±3.84). The maximum nodule diameter was 2.99±0.69 cm, and the disease duration was 1.29±0.34 years. Chronic liver disease was present in 185 patients (84.09%), cirrhosis in 142 patients (64.55%), hepatitis B virus (HBV) infection in 108 patients (49.09%), and alpha-fetoprotein (AFP) levels >200 ng/mL in 120 patients (54.55%).

The benign group comprised 267 patients: 191 males (71.54%) and 76 females, aged 30 to 80 years (mean age: 60.34±5.76). The maximum nodule diameter was 2.50±0.68 cm, and the disease duration was 3.06±0.38 years. Chronic liver disease was present in 102 patients (38.20%), cirrhosis in 68 patients (25.47%), HBV infection in 53 patients (19.85%), and AFP levels >200 ng/mL in 25 patients (9.36%).

Significant differences were found between the malignant and benign groups in clinical indicators such as nodule diameter, disease duration, chronic liver disease, cirrhosis, HBV infection, and AFP levels (all P<0.05). However, no significant differences were observed in gender, metabolic diseases, or previous treatment history (all P>0.05, **Table 2**).

Comparison of CEUS indexes in benign and malignant lesions

The relative blood flow (rBF) in the arterial phase of malignant lesions was significantly greater than that in benign lesions (58.70±4.30 vs. 42.51±4.86, P<0.001), while the rBF in the delayed phase was significantly lower in malignant lesions (17.46±1.48 vs. 18.91±1.25, P< 0.001). Additionally, the initial peak time (11.08±1.15 vs. 14.39±1.47, P<0.001), peak time (34.57±3.82 vs. 45.42±3.79, P<0.001), rise time (25.58±2.60 vs. 37.76±3.29, P< 0.001), kurtosis of the fitted curve (0.39±0.67 vs. 1.15±0.20, P<0.001), and transit time (111.04±12.12 vs. 148.99±13.70, P<0.001) were all significantly shorter in malignant lesions. On the other hand, the perfusion index (145.21±11.21 vs. 89.86±10.55, P<0.001), contrast agent arrival time (3.05±0.57 vs. 2.67±0.52, P<0.001), and peak intensity (10.70±2.12 vs. 4.39±0.91, P<0.001) were significantly higher in malignant lesions compared to benign lesions (**Table 3**).

Comparison of dynamic phase changes in benign and malignant lesions

The dynamic phase change indicators, including initial increase time, initial disappearance time, peak time, and duration, were all significantly lower in malignant lesions than in benign lesions (all P<0.001) (**Table 4**).

Comparison of diagnostic results of different examinations for liver SOLs

For the diagnosis of malignant lesions, the detection rate of CEUS was higher than that of conventional US (75% vs. 43.18%, P<0.001).

Table 2. The demographic data between two groups

	Malignant Group (n=220)	Benign Group (n=267)	P
Age	60.95±3.84	60.34±5.76	0.186
Male (n/%)	162 (73.64%)	191 (71.54%)	0.605
Nodule diameter (cm)	2.99±0.69	2.50±0.68	<0.001
Course of disease (ys)	1.29+0.34	3.06±0.38	<0.001
Chronic liver disease (n/%)	185 (84.09%)	102 (38.20%)	<0.001
Cirrhosis (n/%)	142 (64.55%)	68 (25.47%)	<0.001
Hepatitis B virus infection (n/%)	108 (49.09%)	53 (19.85%)	<0.001
Alpha-fetoprotein >200 ng/mL (n/%)	120 (54.55%)	25 (9.36%)	<0.001
Metabolic disease (n/%)	36 (16.36%)	62 (23.22%)	0.060
Previous treatment history (n/%)	78 (35.45%)	94 (35.21%)	0.954

Table 3. Comparison of CEUS indexes in benign and malignant lesions

	Malignant Group (n=220)	Benign Group (n=267)	t	P
Arterial phase rBF (mL/min)	58.70±4.30	42.51±4.86	38.472	<0.001
Portal phase rBF (mL/min)	28.08±1.20	29.52±2.08	9.061	<0.001
Delayed phase rBF (mL/min)	17.46±1.48	18.91±1.25	11.684	<0.001
Initial peak time (s)	11.08±1.15	14.39±1.47	27.494	<0.001
Peak time (s)	34.57±3.82	45.42±3.79	31.350	<0.001
Rise time (s)	25.58±2.60	37.76±3.29	44.616	<0.001
Transit time (s)	111.04±12.12	148.99±13.70	32.033	<0.001
Perfusion index	145.21±11.21	89.86±10.55	56.021	<0.001
Contrast agent arrival time (s)	3.05±0.57	2.67±0.52	7.569	<0.001
Peak intensity (dB)	10.70±2.12	4.39±0.91	44.057	<0.001
Kurtosis of the fitted curve (l/s)	0.39±0.67	1.15±0.2	53.086	<0.001

CEUS, contrast-enhanced ultrasound; rBF, relative blood flow.

Table 4. Comparison of dynamic phase changes in benign and malignant lesions

Lesion type	Onset time (s)	Peak time (s)	Onset time (s)	Duration (s)
Malignant lesion	12.19±1.54	15.69±1.35	31.56±3.08	40.24±1.46
Benign lesion	21.50±1.40	26.34±3.11	57.46±2.04	135.81±3.16
t	69.871	47.283	110.993	413.943
P	<0.001	<0.001	<0.001	<0.001

Similarly, for benign lesions, the detection rate of CEUS was higher than that of conventional US (80.15% vs. 44.94%, P<0.001) (**Table 5**).

Comparison of diagnostic coincidence rate of diagnosis of lesion size by two examination methods

CEUS showed a higher diagnostic coincidence rate for lesions ≤1 cm compared to conventional US (85.16% vs. 49.47%, P<0.001). However, for lesions sized 1-3 cm and ≥3 cm, the diagnostic coincidence rates between the two methods were not significantly different (P>0.05) (**Table 6**).

Analysis of different inspection results

CEUS demonstrated higher accuracy, sensitivity, specificity, negative predictive value, and positive predictive value compared to conventional US (all P<0.05). A comparison of the optimal cut-off values between conventional US and CEUS showed a significant statistical difference (t=41.499, P<0.001). The cut-off value for conventional US was 0.119, while for CEUS,

Table 5. Comparison of diagnostic results of different examinations for liver space-occupying lesions

Diagnostic examinations	Benign lesion (n=267)	Malignant lesion (n=220)
Contrast-enhanced ultrasound	214 (80.15%)	165 (75%)
Conventional ultrasound	120 (44.94%)	95 (43.18%)
χ^2	70.635	46.068
P	<0.001	<0.001

Table 6. Comparison of the coincidence rate of diagnosis of lesion size by two examination methods

Group	≤1 cm (283 cases)	1-3 cm (124 cases)	≥3 cm (50 cases)
Contrast-enhanced ultrasound	241 (85.16%)	104 (83.87%)	50 (100%)
Conventional ultrasound	140 (49.47%)	99 (79.84%)	47 (94%)
χ^2	81.915	0.679	3.093
P	<0.001	0.410	0.079

Table 7. Analysis of different inspection results

Group	Conventional ultrasound	Contrast-enhanced ultrasound	t	*P*
Accuracy	44.15%	77.82%	24.296	<0.001
Sensitivity	43.18%	75%	21.166	<0.001
Specificity	44.94%	80.15%	26.133	<0.001
Negative predictive value	48.98%	79.55%	20.985	<0.001
Positive predictive value	39.26%	75.69%	28.010	<0.001
Cut-off	0.119	0.551	41.499	<0.001

it was 0.551 (**Table 7**). These results indicate that CEUS has higher diagnostic sensitivity and specificity, with its cut-off value closer to the ideal diagnostic standard, further supporting its superiority in diagnosing liver SOLs.

Typical images of conventional US and CEUS of benign and malignant liver lesions

Benign lesion: Conventional US revealed a nodule measuring approximately 24 × 19 mm in the lower segment of the right anterior lobe of the liver, with a relatively clear boundary, irregular shape, heterogeneous internal echoes, and no acoustic halo. The internal blood flow signal in color Doppler flow imaging (CDFI) was evident (**Figure 2A**). CEUS in the arterial phase showed centripetal hyperenhancement at the center of the nodule. In the portal phase, the lesion showed hyperenhancement with a clear boundary and regular shape. In the delayed phase, the lesion showed slight hyperenhancement (**Figure 2B**).

Malignant lesion: Conventional US showed a mass approximately 64 mm × 44 mm in the upper segment of the left lateral lobe of the liver, with moderately heterogeneous internal echoes, a clear boundary, irregular shape, and no acoustic halo. The internal blood flow signal in CDFI was not prominent (**Figure 2C**). CEUS showed rapid and uniform high enhancement in the arterial phase. In the portal phase, the lesion showed iso-enhancement with indistinct boundaries and irregular shape. In the delayed phase, the lesion exhibited low enhancement (**Figure 2D**).

ROC analysis

The ROC curve analysis showed that the AUC for CEUS in diagnosing liver SOLs was 0.913, significantly higher than that of conventional US (AUC=0.684, P<0.001, calculated using the DeLong test) (**Figure 3**).

Discussion

We analyzed the imaging characteristics of two diagnostic methods. In patients with malignant liver lesions, conventional US typically shows a mass with low internal echo, an unclear boundary, an irregular shape, no acoustic halo, and minimal punctate blood flow signals in CDFI.

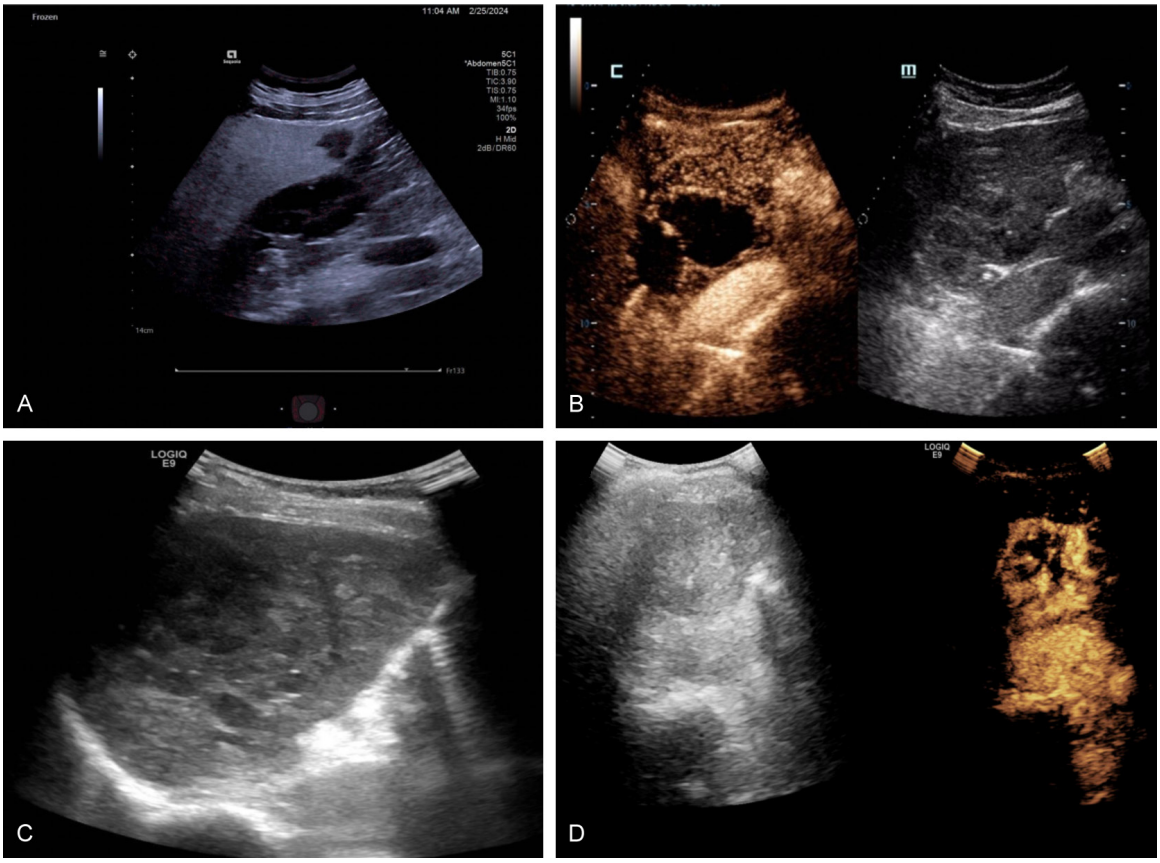

Figure 2. Typical images of conventional ultrasound and CEUS of benign and malignant liver lesions. A: The conventional ultrasound image of the benign lesion. B: The CEUS image of the benign lesion. C: The conventional ultrasound image of the malignant lesion. D: The CEUS image of the malignant lesion. CEUS, contrast-enhanced ultrasound.

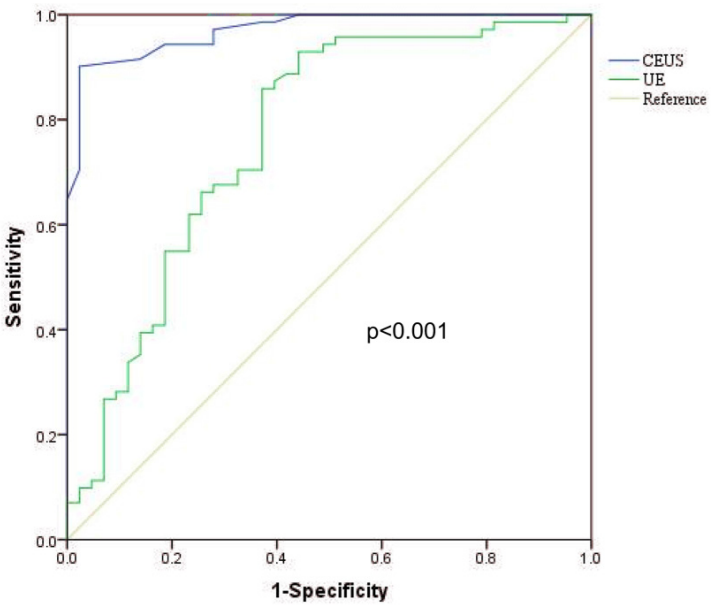

Figure 3. The ROC analysis. ROC, Receiver operating characteristic; CEUS, contrast-enhanced ultrasound; US, ultrasound.

CEUS, in contrast, reveals rapid and uniform high enhancement during the arterial phase. In the portal phase, the lesion demonstrates iso-enhancement with an unclear boundary and irregular shape, while in the delayed phase, low enhancement is observed.

In patients with benign liver lesions, conventional US shows nodules with low internal echo, clear boundaries, regular shape, and no acoustic halo, with an absence of significant internal blood flow signals in CDFI. CEUS reveals a central nodular centripetal hyperenhancement in the arterial phase. In the portal phase, the lesion shows hyperenhancement with clear boundaries and regular

shape, while in the delayed phase, slight hyperenhancement is observed.

Normal liver tissue enhances clearly during the portal phase, while liver cancer shows decreased density and signal, with more obvious decreases in the delayed phase. These findings are consistent with the results of this study.

We then compared the detection rates of the two diagnostic methods for liver cancer, and the results showed that the overall detection rate of CEUS was higher than that of conventional US.

CEUS is a commonly used imaging technique for screening liver lesions [10, 11]. It involves injecting microbubbles into the bloodstream, enhancing the blood flow signal and perfusion intensity within the lesion using second-harmonic imaging technology. This technique allows clear visualization of blood flow signals, helping to differentiate the lesion from surrounding structures and assess its benign or malignant nature [12]. Previous studies have indicated that CEUS has relatively high sensitivity for diagnosing benign and malignant liver lesions [13-17]. In this study, the sensitivity of CEUS in diagnosing benign and malignant focal liver lesions was 88.9%, with a specificity of 96% and an accuracy of 91.3%, consistent with the findings of prior research [13-17]. These results further demonstrate the high efficiency of CEUS in distinguishing the nature of liver SOLs.

CEUS can provide detailed information on the hemodynamic characteristics of liver lesions [18]. Different types of liver lesions exhibit distinct blood supply and perfusion patterns, which CEUS can effectively capture. For instance, malignant lesions typically show rapid enhancement early on, followed by rapid washout in the later stages, while benign lesions tend to have more stable enhancement patterns [19]. Additionally, the microbubbles used in CEUS target the lesion area specifically, interacting with the blood vessels to provide precise details about the vascular structure and function within the lesion. This enhances our understanding of the lesion's nature. Furthermore, CEUS offers high temporal and spatial resolution, enabling real-time and detailed observation of the lesion's enhancement process, which is crucial for accurate diagnosis.

Our findings align with previous studies, which have consistently highlighted the advantages of CEUS in liver lesion characterization. For instance, Li et al. [20] emphasized the ability of CEUS to accurately differentiate HCC from other hepatic lesions based on dynamic perfusion patterns observed during the arterial, portal venous, and late phases. Similarly, Peltec et al. [21] demonstrated that CEUS offers a significant advantage over conventional US in assessing the microvascular characteristics of hepatic lesions, which are critical for distinguishing malignant from benign pathologies. In our study, we observed similar dynamic enhancement patterns, which allowed for precise classification of lesions, corroborating these earlier findings.

However, compared to Yang et al. [22], who reported CEUS sensitivity and specificity values of 88% and 85% for differentiating benign and malignant liver lesions, our study achieved slightly higher diagnostic metrics. This discrepancy may be due to differences in patient populations, lesion characteristics, or study inclusion criteria. For example, our cohort included a higher proportion of smaller or indeterminate lesions, which may have benefited more from the real-time microvascular imaging capabilities of CEUS. Unlike conventional US, CEUS uses microbubble-based contrast agents that remain intravascular, allowing for detailed visualization of microvascular structures and perfusion dynamics [23]. This is particularly important for hepatic lesions, as malignancies often exhibit aberrant vascular patterns, such as arterial-phase hyperenhancement and rapid washout in the portal venous phase. CEUS enables real-time imaging of lesion perfusion, allowing clinicians to observe the entire contrast enhancement process as it unfolds [24]. This capability is especially valuable for lesions with ambiguous characteristics on conventional US. The dynamic assessment of vascular behavior in real time not only improves diagnostic accuracy but also reduces the need for additional imaging.

Unlike CT or MRI, CEUS is radiation-free and non-invasive, making it particularly suitable for patients requiring repeated imaging, such as those with chronic liver disease or during surveillance of at-risk populations [25]. This feature enhances its clinical utility and positions

CEUS as a safer alternative for vulnerable patient groups.

In our study, we also found that CEUS is particularly efficient in differentiating the nature of liver nodules smaller than 1 cm. CEUS clearly shows the microvascular perfusion of these lesions. For small lesions under 1 cm, CEUS can accurately detect the blood flow details in and around the lesion, providing valuable information for assessing the lesion's nature. CEUS helps identify specific enhancement patterns, as different types of liver lesions exhibit characteristic enhancement patterns at different phases. Through careful observation and analysis of these patterns, more accurate judgments can be made [26]. Additionally, the technology allows for real-time dynamic monitoring [27], enabling continuous observation of the lesion's perfusion and washout processes. This is crucial for understanding the characteristics and behavior of small lesions. Furthermore, CEUS's high resolution allows for better distinction of the boundaries and internal structures of small lesions, facilitating a more comprehensive assessment of their properties.

The liver has a dual blood supply from the hepatic artery and portal vein. CEUS allows observation of three vascular phases: the arterial phase, portal venous phase, and delayed phase [28]. By analyzing the enhancement patterns during these phases, different types of liver lesions can be differentiated. CEUS dynamically and in real time reflects the characteristic changes of various liver lesions across these phases, which helps in distinguishing benign from malignant lesions [29, 30]. Our study found that local blood flow in the arterial phase of malignant lesions was significantly higher than in benign lesions, while in the delayed phase, blood flow was significantly lower, indicating clear differences in the blood supply between the two types of lesions. This finding is consistent with previous studies [31-33]. This difference is primarily due to the "rapid in, rapid out" perfusion pattern in malignant tumors, whereas benign tumors exhibit a "rapid in, slow out" pattern. As a result, malignant lesions typically show high enhancement in the arterial phase, followed by a rapid washout in the portal venous and delayed phases [34].

Furthermore, our study revealed that the initial peak time, peak time, rise time, and transit time of malignant lesions were significantly shorter than those of benign lesions, while the perfusion index was significantly higher. This suggests that blood perfusion in malignant lesions is relatively rich. This phenomenon is mainly due to the faster clearance of the contrast agent from malignant tissues compared to benign tissues, as well as the greater number of blood vessels in malignant lesions, which supports increased perfusion [35]. The presence of neovascularization in malignant lesions leads to a relatively richer blood supply. The more abundant the arterial blood supply to liver lesions, the shorter the contrast agent arrival time during CEUS [36, 37].

The clinical application of CEUS in diagnosing liver SOLs holds significant promise, offering several advantages that could transform diagnostic practices in hepatology. With its ability to provide real-time dynamic imaging and superior contrast resolution, CEUS has become a valuable tool for distinguishing between benign and malignant liver lesions. A key advantage of CEUS is its potential for broader adoption as a first-line diagnostic tool. Compared to traditional imaging methods like CT and MRI, CEUS is less invasive, radiation-free, and more cost-effective. These qualities make it particularly suitable for routine diagnostics, follow-up evaluations, and for patient populations requiring frequent imaging, such as those with chronic liver diseases or a history of HCC.

Furthermore, advancements in contrast agents and imaging technologies are expected to further enhance the diagnostic accuracy of CEUS. The development of next-generation contrast agents with better safety profiles and longer retention times in the vascular system could improve the visualization of lesion microvascular structures, enabling more precise characterization of tumor perfusion patterns. Additionally, integration with artificial intelligence (AI) and machine learning algorithms has the potential to standardize image interpretation, reduce operator dependence, and improve diagnostic consistency across various clinical settings.

In personalized medicine, CEUS may also play a crucial role in tailoring treatment strategies for patients with liver lesions. By providing detailed information on vascularization and perfusion, CEUS can assist in determining the suitability of specific interventions such as transarterial

chemoembolization (TACE), radiofrequency ablation (RFA), or systemic therapies. Moreover, its real-time monitoring of therapeutic response offers opportunities to optimize treatment protocols and improve patient outcomes.

Despite its promising prospects, several challenges must be addressed to fully realize the potential of CEUS in clinical practice. Standardization of diagnostic criteria, particularly for complex lesions, remains an important area for future research. Large-scale multicenter studies and clinical trials are needed to validate its efficacy and reproducibility across diverse patient populations. Additionally, the availability of CEUS expertise and training programs for healthcare professionals must be expanded to ensure widespread and effective implementation.

The clinical value of CEUS in diagnosing liver SOLs is substantial, with the potential to improve diagnostic accuracy, optimize therapeutic strategies, and enhance overall patient management. With ongoing technological advancements and efforts to address current limitations, CEUS is poised to play an increasingly pivotal role in hepatology and liver disease management.

This study has several limitations. First, its retrospective design introduces potential selection bias. Second, the sample size of patients with liver carcinoma was small, and some patients did not meet the inclusion criteria. Third, comparative analysis with other imaging methods, such as enhanced CT or MRI, was not included. Additionally, while the study focused on evaluating the diagnostic performance of CEUS for liver SOLs based on imaging characteristics, the retrospective nature of the data and incomplete pathological and prognostic parameters limited further analysis. Future prospective studies should include detailed pathological data and long-term follow-up to better understand the relationship between CEUS findings, pathological features, and patient prognosis.

In conclusion, CEUS is effective for diagnosing liver SOLs, with higher sensitivity and specificity than conventional US, making it a highly valuable tool in clinical diagnostics.

Disclosure of conflict of interest

None.

Address correspondence to: Yuanyuan Jiang, Department of Ultrasound Medicine, Shandong Second Provincial General Hospital, No. 4, Duanxing West Road, Huaiyin District, Jinan 250022, Shandong, China. Tel: +86-0531-83086230; E-mail: jiangyuanyuan15@163.com

References

[1] Vasireddy R, Bilalaga MM, Iding J and Sankineni A. Challenges in diagnosis: primary hepatic lymphoma presenting as a space-occupying liver lesion. ACG Case Rep J 2024; 11: e01443.

[2] Gingold-Belfer R, Shinhar N, Bachar GN, Issa N, Boltin D, Sharon E, Shohat T, Sapoznikov B, Swartz A, Peleg N, Konikoff T and Schmilovitz-Weiss H. Predictors of poor outcome following liver biopsy for the investigation of new hepatic space occupying lesion/s. Clin Imaging 2023; 99: 19-24.

[3] Qin Y, Tang C, Li J and Gong J. Liver cancer in China: the analysis of mortality and burden of disease trends from 2008 to 2021. BMC Cancer 2024; 24: 594.

[4] Zhao NB, Chen Y, Xia R, Tang JB and Zhao D. Prognostic value of ultrasound in early arterial complications post liver transplant. World J Gastrointest Surg 2024; 16: 13-20.

[5] Wang C, Jiang H, Zhu J and Jin Y. A new agent for contrast-enhanced intravascular ultrasound imaging in vitro: polybutylcyanoacrylate nanoparticles with drug-carrying capacity. Artif Cells Nanomed Biotechnol 2024; 52: 218-228.

[6] Cotter B, Raisinghani A and DeMaria AN. Established and emerging roles for ultrasound enhancing agents (contrast echocardiography). Clin Cardiol 2022; 45: 1114-1122.

[7] Rónaszéki AD, Dudás I, Zsély B, Budai BK, Stollmayer R, Hahn O, Csongrády B, Park BS, Maurovich-Horvat P, Győri G and Kaposi PN. Microvascular flow imaging to differentiate focal hepatic lesions: the spoke-wheel pattern as a specific sign of focal nodular hyperplasia. Ultrasonography 2023; 42: 172-181.

[8] Delaney LJ, Tantawi M, Wessner CE, Machado P, Forsberg F, Lyshchik A, O'Kane P, Liu JB, Civan J, Tan A, Anton K, Shaw CM and Eisenbrey JR. Predicting long-term hepatocellular carcinoma response to transarterial radioembolization using contrast-enhanced ultrasound: initial experiences. Ultrasound Med Biol 2021; 47: 2523-2531.

[9] Guo J, Jiang D, Qian Y, Yu J, Gu YJ, Zhou YQ and Zhang HP. Differential diagnosis of different types of solid focal liver lesions using two-dimensional shear wave elastography. World J Gastroenterol 2022; 28: 4716-4725.

[10] Zhou G, Zhang Y, You Y, Wang B, Wang S, Yang C, Zhang Y and Liu J. Contrast-enhanced ultrasound and magnetic resonance enhancement based on machine learning in cancer diagnosis in the context of the internet of things medical system. Comput Intell Neurosci 2022; 2022: 4378173.
[11] Kang HJ, Lee JM and Kim SW. Sonazoid-enhanced ultrasonography for noninvasive imaging diagnosis of hepatocellular carcinoma: special emphasis on the 2022 KLCA-NCC guideline. Ultrasonography 2023; 42: 479-489.
[12] Squires JH, Fetzer DT and Dillman JR. Practical contrast enhanced liver ultrasound. Radiol Clin North Am 2022; 60: 717-730.
[13] He H, Wu X, Jiang M, Xu Z, Zhang X, Pan J, Fu X, Luo Y and Chen J. Diagnostic accuracy of contrast-enhanced ultrasound synchronized with shear wave elastography in the differential diagnosis of benign and malignant breast lesions: a diagnostic test. Gland Surg 2023; 12: 54-66.
[14] Liu Q, Gong H, Chen Q, Yuan C and Hu B. Clinical application value of contrast-enhanced ultrasound in the diagnosis of renal space-occupying lesions. Int J Nephrol Renovasc Dis 2023; 16: 253-259.
[15] Açar ÇR and Orguc S. Comparison of performance in diagnosis and characterization of breast lesions: contrast-enhanced mammography versus breast magnetic resonance imaging. Clin Breast Cancer 2024; 24: 481-493.
[16] Chen XJ, Huang LJ, Mao F, Yuan HX, Wang X, Lu Q and Dong CH. Value of CEUS features in diagnosing thyroid nodules with halo sign on B-mode ultrasound. BMC Med Imaging 2023; 23: 11.
[17] Urhuț MC, Săndulescu LD, Ciocâlteu A, Cazacu SM and Dănoiu S. The clinical value of multimodal ultrasound for the differential diagnosis of hepatocellular carcinoma from other liver tumors in relation to histopathology. Diagnostics (Basel) 2023; 13: 3288.
[18] Chen H, Mirg S, Gaddale P, Agrawal S, Li M, Nguyen V, Xu T, Li Q, Liu J, Tu W, Liu X, Drew PJ, Zhang N, Gluckman BJ and Kothapalli SR. Multiparametric brain hemodynamics imaging using a combined ultrafast ultrasound and photoacoustic system. Adv Sci (Weinh) 2024; 11: e2401467.
[19] Taiji R, Cortes AC, Zaske AM, Williams M, Dupuis C, Tanaka T, Nishiofuku H, Chintalapani G, Peterson CB and Avritscher R. Liver cancer vascularity driven by extracellular matrix stiffness: implications for imaging research. Invest Radiol 2023; 58: 894-902.
[20] Li W, Lv XZ, Zheng X, Ruan SM, Hu HT, Chen LD, Huang Y, Li X, Zhang CQ, Xie XY, Kuang M, Lu MD, Zhuang BW and Wang W. Machine learning-based ultrasomics improves the diagnostic performance in differentiating focal nodular hyperplasia and atypical hepatocellular carcinoma. Front Oncol 2021; 11: 544979.
[21] Peltec A and Sporea I. Multiparametric ultrasound as a new concept of assessment of liver tissue damage. World J Gastroenterol 2024; 30: 1663-1669.
[22] Yang J, Huang J, Zhang Y, Zeng K, Liao M, Jiang Z, Bao W and Lu Q. Contrast-enhanced ultrasound and contrast-enhanced computed tomography for differentiating mass-forming pancreatitis from pancreatic ductal adenocarcinoma: a meta-analysis. Chin Med J (Engl) 2023; 136: 2028-2036.
[23] Sridharan A, Eisenbrey JR, Forsberg F, Lorenz N, Steffgen L and Ntoulia A. Ultrasound contrast agents: microbubbles made simple for the pediatric radiologist. Pediatr Radiol 2021; 51: 2117-2127.
[24] Ricci P, Cantisani V, Ballesio L, Pagliara E, Sallusti E, Drudi FM, Trippa F, Calascibetta F, Erturk SM, Modesti M and Passariello R. Benign and malignant breast lesions: efficacy of real time contrast-enhanced ultrasound vs. magnetic resonance imaging. Ultraschall Med 2007; 28: 57-62.
[25] Kim S, Chughtai K, Brahmbhatt A, Rubens D and Dogra V. Contrast-enhanced ultrasound as a problem-solving modality: tips and tricks. Ultrasound Q 2022; 38: 103-115.
[26] Philipp J, Schmidberger J, Schlingeloff P and Kratzer W. Differentiation of hepatic alveolar echinococcosis with a hemangioma-like pattern compared to typical liver hemangioma using contrast-enhanced ultrasound: a pilot study. Infection 2023; 51: 159-168.
[27] Wang W, Liu JY, Yang Z, Wang YF, Shen SL, Yi FL, Huang Y, Xu EJ, Xie XY, Lu MD, Wang Z and Chen LD. Hepatocellular adenoma: comparison between real-time contrast-enhanced ultrasound and dynamic computed tomography. Springerplus 2016; 5: 951.
[28] Baldini G, Hosch R, Schmidt CS, Borys K, Kroll L, Koitka S, Haubold P, Pelka O, Nensa F and Haubold J. Addressing the contrast media recognition challenge: a fully automated machine learning approach for predicting contrast phases in CT imaging. Invest Radiol 2024; 59: 635-645.
[29] Trenker C, Kunsch S, Michl P, Wissniowski TT, Goerg K and Goerg C. Contrast-enhanced ultrasound (CEUS) in hepatic lymphoma: retrospective evaluation in 38 cases. Ultraschall Med 2014; 35: 142-148.
[30] Ma AD, Zhang Y, Xue Z and Li K. Angiogenesis of hepatocellular carcinoma under multislice

spiral CT plain scan and enhanced scan. J Biol Regul Homeost Agents 2015; 29: 895-903.
[31] Aziz MU, Eisenbrey JR, Deganello A, Zahid M, Sharbidre K, Sidhu P and Robbin ML. Microvascular flow imaging: a state-of-the-art review of clinical use and promise. Radiology 2022; 305: 250-264.
[32] Takumi K, Nagano H, Kikuno H, Kumagae Y, Fukukura Y and Yoshiura T. Differentiating malignant from benign salivary gland lesions: a multiparametric non-contrast MR imaging approach. Sci Rep 2021; 11: 2780.
[33] Dong Y, Wang WP, Ignee A, Zuo D, Qiu YJ, Zhang Q, Lu XY, Chen S and Dietrich CF. The diagnostic value of Doppler Resistive Index in the differential diagnosis of focal liver lesions. J Ultrason 2023; 23: e45-e52.
[34] Burrowes DP, Medellin A, Harris AC, Milot L and Wilson SR. Contrast-enhanced US approach to the diagnosis of focal liver masses. Radiographics 2017; 37: 1388-1400.
[35] Ying L, Luo L, Li F, Zhou H, Tao X and Ling Y. Quantitative perfusion analysis of contrast-enhanced ultrasound might help differentiate benign and malignant solid cystic lesions of the kidney: a case report and literature review. Curr Med Imaging 2024; 20: 1-5.
[36] Gao X, Tang H, Wang J, Yao Q, Wang H, Wang Y, Ma M, Yang W, Yan K and Wu W. Specific imaging features indicate the clinical features of patients with hepatic perivascular epithelioid cell tumor by comparative analysis of CT and ultrasound imaging. Front Oncol 2022; 12: 908189.
[37] Li Q, Nie F, Yang D, Dong T and Liu T. Contrast-enhanced ultrasound (CEUS) - a new tool for evaluating blood supply in primary peripheral lung cancer. Clin Hemorheol Microcirc 2023; 83: 61-68.